# A first assessment of the SMOS data in southwestern France using in situ and airborne soil moisture estimates : the CAROLS airborne campaign

Clément Albergel, Elena Zakharova, Jean-Christophe Calvet, Mehrez Zribi, Mickaël Pardé, Jean-Pierre Wigneron, Nathalie Novello, Yann H. Kerr, Arnaud Mialon, Nour-Ed-Dine Fritz

# A first assessment of the SMOS data in southwestern France using in situ and airborne soil moisture estimates: the CAROLS airborne campaign

Clément Albergel[1,2], Elena Zakharova[1], Jean-Christophe Calvet[1], Mehrez Zribi[3-4], Mickaël Pardé[4], Jean-Pierre Wigneron[5], Nathalie Novello[5], Yann Kerr[3], Arnaud Mialon[3], Nour-ed-Dine Fritz[1]

[1] CNRM-GAME, Météo-France, CNRS, URA 1357, 42 avenue Gaspard Coriolis, Toulouse, France,

[2] Now at ECMWF, Shinfield Park, Reading UK,

[3] CESBIO, CNES/CNRS/IRD/UPS, UMR 5126, 18 Avenue Edouard Belin, Toulouse, France,

[4] LATMOS/CNRS, 10-12 av. de l'Europe, Vélizy, France

[5] INRA, EPHYSE, 71 avenue Edouard Bourlaux, Villenave d'Ornon, France,

Correspondence to: J.-C. Calvet (jean-christophe.calvet@meteo.fr)

**Abstract -** The Soil Moisture and Ocean Salinity (SMOS) satellite mission, based on an aperture synthesis L-band radiometer was successfully launched in November 2009. In the context of a validation campaign for the SMOS mission, intensive airborne and in situ observations were performed in southwestern France for the SMOS CAL/VAL, from April to May 2009 and from April to July 2010. The CAROLS (Cooperative Airborne Radiometer for Ocean and Land Studies) bi-angular (34°-0°) and dual-polarized (V and H) L-band radiometer was designed, built and installed on board the French ATR-42 research aircraft. During springs of 2009 and 2010, soil moisture observations from the SMOSMANIA (Soil Moisture

Observing System – Meteorological Automatic Network Integrated Application) network of Météo-France were complemented by airborne observations of the CAROLS L-band radiometer, following an Atlantic-Mediterranean transect in southwestern France. Additionally to the 12 stations of the SMOSMANIA soil moisture network, in situ measurements were collected in three specific sites within an area representative of a SMOS pixel. Microwave radiometer observations, acquired over southwestern France by the CAROLS instrument were analyzed in order to assess their sensitivity to surface soil moisture ($w_g$). A combination of microwave brightness temperature ($T_b$) at either two polarizations or two contrasting incidence angles was used to retrieve $w_g$ through regressed empirical logarithmic equations with good results, depending on the chosen configuration. The regressions derived from the CAROLS measurements were applied to the SMOS $T_b$ and their retrieval performance was evaluated. The retrievals of $w_g$ showed significant correlation ($p$-value $< 0.05$) with surface measurements for most of the SMOSMANIA stations (8 of 12 stations) and with additional field measurements at two specific sites, also. Root mean square errors varied from 0.03 to 0.09 $m^3m^{-3}$ (0.06 $m^3m^{-3}$ on average).

# 1. Introduction

Soil moisture controls both evaporation and transpiration from bare soil and vegetated areas, respectively, playing a key role in the interactions between the hydrosphere, the biosphere and the atmosphere. As a consequence, a significant amount of studies have been and are currently conducted to obtain soil moisture estimates. For that purpose, land surface modeling (Dirmeyer et al., 1999, Georgakakos and Carpenter 2006 among others) and remote sensing techniques (Wagner et al., 1999, 2007; Kerr et al., 2001, 2007; Njoku et al., 2003) are used. Indeed, microwave remote sensing is able to provide quantitative information about the water content of a shallow near surface layer (Schmugge, 1983), particularly in the low-frequency microwave region from 1 to 10 GHz. Passive microwave remote sensing of soil moisture has been at the center of attention of many research programs, for several decades. Various airborne and in situ radiometers have been developed, showing the high potential of L-band (1.41 GHz) measurements for the estimation of surface parameters (Skou, 1989, Wilson et al., 2001, Le Maitre et al., 2004). Whereas it was shown that surface soil moisture influences the microwave emission of relatively dense vegetation canopies from L-band to K-band (~1.41–23.8 GHz, e.g. Calvet et al., 2011), L-band is the optimal wavelength range to observe soil moisture (e.g. Wigneron et al., 1995). Higher frequencies are more significantly affected by perturbing factors such as atmospheric effects and vegetation cover (Schmugge, 1983, Kerr et al., 2001). At L-band, soil moisture in the first centimetres of soil impacts significantly on the emitted brightness temperature through a straightforward link between $T_b$ and $w_g$, about 2 K per 1% of volumetric soil moisture over bare soil (Schmugge and Jackson, 1994, Chanzy et al., 1997).

From a satellite point of view, apart from a few days of L-band radiometric observations on Skylab between June 1973 and January 1974 (Jackson et al., 2004) current or past instruments have been operating at frequencies above 5 GHz. The Soil Moisture and Ocean Salinity mission (SMOS), is the first dedicated soil moisture mission launched in November 2009 (Kerr et al., 2001, 2007). It consists of a spaceborne L-band (~1.42 GHz, 21 cm) interferometric radiometer using L-band radiometry able to provide multiangular microwave polarimetric brightness temperature ($T_b$) and soil moisture product ($w_g$). Wigneron et al. (1995, 2003), have shown that it is possible to retrieve biophysical variables from bipolarized and multiangular microwave $T_b$, including soil moisture. In the context of a validation campaign for the SMOS mission, the CAROLS L-Band (Cooperative Airborne Radiometer for Ocean and Land Studies) radiometer was designed, built and operated from an aircraft. The first CAROLS flights started in September 2007, for the qualification and certification of the instrument. Following various improvements to the CAROLS instrument, a second campaign was carried out in November 2008, in order to validate the CAROLS's data quality (Zribi et al., 2010). In the springs of 2009 and 2010, two scientific campaigns were organized, to acquire different types of brightness measurements over oceanic and land surfaces. This study focuses on land surface observations with several flights over the twelve stations of the SMOSMANIA (Soil Moisture Observing System – Meteorological Automatic Network Integrated Application) soil moisture network of Météo-France (Calvet et al., 2007, Albergel et al., 2008). SMOSMANIA consists in a long term data acquisition effort of profile soil moisture observations in southern France. The SMOSMANIA network was already used to assess soil moisture estimates from either remote sensing (Albergel et al., 2009) or numerical weather prediction models (Albergel et al., 2010). Additional in situ measurements were performed in 2009 and 2010, also, in three areas located within a SMOS pixel.

In this study, the two CAROLS campaigns of 2009 and 2010 over southwestern France are presented. The sensitivity of the CAROLS's $T_b$ measurements to soil moisture is investigated. The $T_b$ are compared to the in situ measurements of soil moisture, from the SMOSMANIA network and from the above mentioned additional measurements sites. Regressed empirical logarithmic equations are used to retrieve soil moisture from $T_b$ observations. The retrieval performance of the regression (Calvet et al. 2011) is used as an indicator of the sensitivity of the CAROLS microwave to soil moisture and applied to SMOS data. After a description of the CAROLS airborne campaign and of the different soil moisture data sets used in this study, a short section describes the SMOS brightness temperatures. Then, a methodology for the evaluation the CAROLS data is presented, as well as the soil moisture retrieval method. Finally, the results are presented and discussed.

# 2. Material and methods

## *2.1. CAROLS observations*

### 2.1.1. Flight description

During the two scientific campaigns of springs 2009 and 2010, the CAROLS instrument onboard the research ATR-42 aircraft (Zribi et al. 2011), acquired L-band $T_b$ (in conjunction with other measurements like infrared temperature) over the SMOSMANIA network, in southwestern France. Twenty-four flights were performed, at 2000m above sea level (asl): 6 in 2009 and 18 in 2010. For some of them, manual measurements of soil moisture were made, in addition to the automated measurements of the SMOSMANIA network. Table 1 provides details of the two CAROLS campaign flights and Fig. 1 shows an overview of the flights. The studied flights covered either the whole transect over the SMOSMANIA network or the western part of the transect. The latter corresponded to ocean flights over the gulf of Biscay.

All the flights started from Toulouse, and observations were made from Toulouse to the gulf of Biscay and vice versa. The complete SMOSMANIA flights included an additional flight line from Toulouse to the Mediterranean sea and vice versa. A complete SMOSMANIA flight was performed in about 3 hours.

### 2.1.2. CAROLS L-band radiometric observations

CAROLS is a total power radiometer and has a simple structure and high theoretical sensitivity. The receiver was developed as a copy of the EMIRAD II radiometer, in collaboration between the DTU (Danish Technical University) and LATMOS (Laboratoire Atmosphères, Milieux, Observations Spatiales) laboratory. It is a fully polarimetric correlation radiometer using direct sampling, performing biangular (34°-0°) and bipolarized (V and H polarizations) observations. Two antennas provide dual–incidence measurements, useful for the estimation of soil moisture (Wigneron et al., 2004) or ocean salinity from brightness temperatures. The microwave emission of the surface is observed at two incidence angles, nadir (0°) and 34° (slant side-looking antenna). Considering a flight height of about 2000m asl, the antenna spotting at nadir observes an area of 1362m large and the side looking antenna observes an area of 2062m large. In this configuration, given the simple straight-line flights at 2000m asl and the overlaid of both nadir and side looking antenna, the CAROLS instrument observes a corridor of about 3km, presented in Fig. 2. More information is available in Zribi et al. (2011). The radiometer was installed in the French research ATR-42 aircraft in conjunction with other airborne instruments (C-Band scatterometer (STORM), the GOLD-RTR GPS system, the Infrared CIMEL radiometer and a visible wavelength camera). The CAROLS radiometer was validated and qualified with laboratory measurements (Zribi et. al., 2011). The infrared radiometer is part of the standard equipment of the research ATR-42. This instrument points to nadir, and has a 3° field of view. It measures the thermal emission of the Earth's surface in three channels, 8.7, 10.8 and 12 µm, respectively. It is used to provide surface temperature estimations, simultaneously with the CAROLS measurements.

Radio Frequency Interferences (RFI) were observed by CAROLS along the SMOSMANIA transect (Zribi et al., 2011 ; Pardé et al., 2011). Passive radiometers are particularly susceptible to artificial microwave emissions (Njoku et al., 2005). The main sources responsible for most of the RFI were identified (Pardé et al. 2011). They correspond to antennas with an emission frequency within or spilling into the protected L-band used by both CAROLS and SMOS instruments. The identified RFI areas were suppressed from the data used in this study, as in Zribi et al. (2011). However, residual low RFI perturbations may remain in the data set.

### 2.2. In situ soil moisture: the SMOSMANIA network and manual measurements

The main objective of the SMOSMANIA network is to validate remotely sensed soil moisture. However the use of observations obtained from SMOSMANIA is not limited to satellite validation and other objectives include: (i) the validation of the operational soil moisture products of Météo-France, produced by the hydrometeorological SIM model (Habets et al., 2005, 2008), (ii) the validation of new versions of the ISBA land surface model of Météo-France, (iii) ground-truthing of airborne Cal/Val campaigns in support of the SMOS mission and (iv) the evaluation of remotely sensed soil moisture products.

The SMOSMANIA network is based on the existing automatic weather station network of Météo-France (RADOME, Réseau d'Acquisition de Données d'Observations Météorologiques Etendues). In 2006, twelve stations of the RADOME network in Southwestern France were equipped with soil moisture probes at four depths (5, 10, 20 and 30 cm). The RADOME stations observe air temperature and relative humidity, wind speed and precipitation. Downwelling shortwave radiation is also measured at some stations. The twelve stations of the SMOSMANIA network are located along a 400 km transect between the Mediterranean Sea and the Atlantic Ocean following the climatic gradient between the two coastlines. The three most westward and the three most eastward stations are located in areas with a high fraction of forests, either temperate or Mediterranean, respectively. The six stations at the centre of the transect, Peyrusse-Grande, Condom, Lahas, Savenes, Montaut, and Saint-Félix de Lauragais (PRG, CDM, LHS, SVN, MNT, and SFL, respectively), are located in areas dominated by croplands. The soil moisture measurements are in units of $m^3m^{-3}$, they are derived from capacitance probes: ThetaProbe ML2X of Delta-T Devices, easily interfaced with the RADOME stations. A ThetaProbe provides a signal in units of volt and its variations is virtually proportional to changes in the soil moisture content over a large dynamic range (White et al., 1994). In this study, in order to convert the voltage signal into a volumetric soil moisture content, site-specific calibration curves were developed using in situ gravimetric soil samples, for each station, and each depth i.e., 48 calibrations curves (Calvet et al., 2007; Albergel et al., 2008). The ThetaProbes were installed in 2006 and have produced continuous observations since then, with a sampling time of 12 min. In this study, data acquired in 2010 are used. Along with soil moisture measurements, soil temperature is measured, also.

While SMOSMANIA was mainly designed to support the validation of soil moisture estimates from SMOS, other satellite-derived surface soil moisture products may be considered, together with model soil moisture estimates over France (Rüdiger et al., 2009; Albergel et al., 2009, 2010), e.g. AMSR-E (Advanced Microwave Scanning Radiometer for Earth Observing System), WindSAT (a multi-frequency polarimetric microwave radiometer), or the C-band ASCAT (Advanced Scatterometer) instrument. Figure 1 shows the SMOSMANIA network in southwestern France. The Lézignan-Corbières (LZC) station is not used in this study as no data were observed for most of the 2010 period due to technical problems.

In addition to the twelve stations of the SMOSMANIA network, soil moisture was measured at three transects within an area representative of a SMOS pixel, at the east of the LHS station. These observations were performed in order to characterize the heterogeneity of the pixel. The transects are presented in Fig. 3. The first one (Le Mona) is representative of an hilly agricultural area with mixed crops, the second one (Lahage) corresponds to a forest and the third one (Berat) is a flat agricultural area with maize. Soil moisture was sampled within the three sites, under the flight track in conjunction with the CAROLS flights. Measurements were performed using Thetaprobes, as used for the the SMOSMANIA stations, providing a signal in units of volt. A calibration curve was developed to convert the voltage into volumetric soil moisture content ($m^3m^{-3}$). The calibration was performed in situ through regular gravimetric samples over the three sites. 90 gravimetric measurements were acquired in 2009 allowing the determination of a calibration curve with an accuracy of about 0.03 $m^3m^{-3}$. Figure 4 presents an illustration of the soil moisture data sampled at the Le Mona site for 28 April 2010.

### *2.3. SMOS brightness temperatures*

Brightness temperature and soil moisture from SMOS mission are also used in this study. One of the main objectives of SMOS is the mapping of global surface soil moisture with an accuracy better than 0.04 $m^3$ $m^{-3}$, every three days (Kerr et al., 2001). The 2-D interferometric radiometer allows measuring $T_b$ at many incidence angles, and is fully polarized. Over land surfaces, the sensitivity of individual SMOS $T_b$ observations at a given location ranges between 2.5 and 4K. While such high noise levels are detrimental to soil moisture retrieval (Pellarin et al. 2003a), the use of several $T_b$ values, at two polarizations and for several incidence angles, permits to cope with this problem.

In this study, the $T_b$V and $T_b$H at an incidence angle of 34° (consistent with the incidence angle of the $T_b$ observed by the CAROLS slant antenna) were extracted for the different studied sites, from L1c SMOS product provided to CAL/VAL teams by ESA. They corresponded to data before any reprocessing, i.e., with faults in the calibration and inconsistencies in the processing (due to the commissioning phase activities). Results are thus to be considered with caution. Valid SMOS observations close to nadir were scarce, and $T_b$ values at 34° were considered, only. First, the $T_b$ were corrected for the Faraday rotation induced by the ionosphere and recalculated from the antenna (X, Y polarizations) to the Earth surface (H and V polarizations) reference frame. Second, $T_b$V and $T_b$H median values were calculated in a range of incidence angles of 34° ± 2°. The SMOS observations over France are subjected to RFI, and in southwestern France, the most affected area is the Atlantic part of the CAROLS transect. In order to remove contaminated measurements, the data were filtered. The filter criterion used for SMOS $T_b$ was based on halved first Stokes parameter calculated as $T_b$S1 = 0.5*( $T_b$H+ $T_b$V) (Kerr et al., 2007). The $T_b$ measurements out of a two standard deviation interval were considered to be contaminated by RFI. The mean value and standard deviation of $T_b$S1 were calculated for the March-July 2010 period over the France domain.

### 2.4. Methodology

For each station of the SMOSMANIA network, CAROLS $T_b$ are averaged within a 20 km radius around the station, consistent with the scale of a SMOS pixel (~40 km), and compared to soil moisture observations. When considering the 3 additional sites, they are averaged within a 1 km radius to be compared with in situ observations and within 20 km to be compared with the soil moisture as seen by SMOS. Retrieving soil moisture from microwave $T_b$, Wigneron et al. (2004) have shown that the τ-ω model (Wigneron et al., 1995) can be used to build semi-empirical statistical relationships between $w_g$ and microwave reflectivities observed at two contrasting incidence angles. These relationships could, potentially, be used for $w_g$ and vegetation optical thickness retrieval. Saleh et al. (2006), presented a review of index-based methods and semi-empirical regression methods at L-band. They consist of either single configurations (one incidence angle, one polarization) or multiple configurations (one polarization and two angles, or two polarizations and one angle). Saleh et al. (2006) demonstrated that better $w_g$ retrievals are obtained with the multiple configuration regression (either biangular or bipolarization). In addition to soil moisture, it is possible to retrieve the vegetation water content (VWC) and the optical depth of the canopy (which depends on the VWC). This study focuses on $w_g$ retrieval, and the multiple configuration regression method used to assess the sensitivity of the CAROLS's microwave observations to $w_g$ at different frequencies is presented by Eq.(1a). Eq.(1a) was used by Calvet et al. (2011), adapted from Saleh et al. (2006).

$$w_g = \exp\left( A_{w_g} \ln\left(1 - \frac{T_b(\theta_1, p)}{T_{IR}}\right) + B_{w_g} \ln\left(1 - \frac{T_b(\theta_2, q)}{T_{IR}}\right) + c_{w_g} \right) \qquad \text{Eq.(1a)}$$

Eq.(1a) is used with CAROLS data in three configurations, two biangular ($\theta_1 \neq \theta_2$, p=q, i.e. 34H0H and 34V0V) and one bipolarized ($\theta_1 = \theta_2$, p≠q, i.e. 34VH) configurations. Following Saleh et al. (2006), the regression coefficients $A_{wg}$, $B_{wg}$, $C_{wg}$ may vary from one configuration to another. As in Calvet et al. (2011) the regression coefficients are based on $w_g$ observations from either the SMOSMANIA network or additional measurements, $T_b$ and surface temperature estimates. The use of the airborne infrared temperature observations ($T_{IR}$) would limit the analysis of the empirical coefficients to the CAROLS flight times. Indeed, the availability of the SMOS data is not restricted to the CAROLS flight times. Therefore, an effective temperature ($T_{eff}$) based on the SMOSMANIA soil temperature profiles were used instead of $T_{IR}$, for both CAROLS and SMOS $T_b$:

$$w_g = \exp\left( A_{w_g} \ln\left(1 - \frac{T_b(\theta_1, p)}{T_{eff}}\right) + B_{w_g} \ln\left(1 - \frac{T_b(\theta_2, q)}{T_{eff}}\right) + c_{w_g} \right) \qquad \text{Eq.(1b)}$$

The simple method of estimation of $T_{eff}$ uses measured or simulated ground temperatures ($T_{gr}$) at the different depth. The simple approach developed by Choudhury (Choudhury et al., 1982) to estimate $T_{eff}$ consists of using two soil temperatures: at depth ($T_{depth}$) and at the surface ($T_{surf}$).

$$T_{eff} = T_{depth} + (T_{surf} - T_{depth})\,C_t \qquad \text{Eq.(2)}$$

where $C_t$ depends on frequency (L-band in this study). While Choudhury et al. (1982) use $C_t$ = 0.246 at L-band, Wigneron et al. (2008) developed and tested more complex formulations that account for the dependence of $C_t$ on soil moisture and soil texture - clay and sand content. In this study, soil temperature values measured by the SMOSMANIA stations are used: $T_{surf}$ at 5cm and $T_{depth}$ at 30 cm. As a preliminary analysis showed no significant added value of the most complex approaches on the results of this study, the results obtained using the simple Choudhury approach are shown, only. Moreover, it was checked (not shown) that the higher $C_t$ values given by Wigneron et al. (2008) for Eq. (2), ranging from 0.5 to 1, tend to reduce the number of usable $T_b$ values in Eq. (1b), as $T_{eff}$ values are higher. Finally, $C_t$ = 0.246 was used.

In a first attempt to test the sensitivity of CAROLS microwave observations to $w_g$, three scores are considered: the correlation (r), the root mean square error (RMSE) and the Fisher's *F*-test *p*-value. The *p*-value indicates the significance of the test, if it is small (e.g. below 0.05), it means that the correlation is not a coincidence. In this study, the following thresholds on *p*-values are used: (i) NS (non significant) for *p*-value greater than 0.05, (ii) * between 0.05 and 0.01, (iii) ** between 0.01 and 0.001, (iv) *** between 0.001 and 0.0001 and (v) **** below a value of 0.0001.

# 3. Results

## 3.1. Sensitivity of CAROLS $T_b$ to $w_g$

As an illustration of the CAROLS $T_b$ response to surface soil moisture, Fig. 5 presents CAROLS's microwave observations (dots) at nadir (0°) in vertical polarization (V) with errors bars (standard deviation) for two neighboring stations (less than 40 km apart) of the SMOSMANIA network. Precipitation is presented, also. On the basis of Fig. 5, it is possible to appreciate the response of $T_b$ to rain events (i.e. to rises in surface soil moisture). The precipitation events correspond to reduced $T_b$, whereas the drying out following the precipitation events corresponds to increases in $T_b$. The strong link between L-band $T_b$ and $w_g$ is demonstrated by Table 2, presenting the correlation between $T_b$ (in four configurations, nadir and slant in both H and V polarization) and $w_g$. Regarding the SMOSMANIA network, scores are better with $T_b$ at nadir, with correlations ranging from -0.526 to -0.878, at either vertical or horizontal polarization, with an average of –0.76. $T_b$ at slant present lower correlations, ranging from –0.169 to –0.494 (with an average of –0.30) and –0.241 to –0.737 (with an average of –0.58), at V and H polarization, respectively. For Le Mona, Lahage and Berat sites, average correlations greater than –0.82 are obtained (see Table 2), except for CAROLS $T_b$ at slant (34°) V polarization which presents low correlations (-0.208 on average).

Figure 6 presents, for each station of the SMOSMANIA network, and for the three additional sites, the CAROLS microwave observations (nadir, V polarization) as a function of soil moisture for 2009 and 2010. More often than not, tendencies observed for both 2009 and 2010 are similar. However, the Le Mona case is of interest. While $T_b$ values observed in 2009 are in the same range as those observed in 2010, the observed $w_g$ were higher in 2009. Indeed, the L-band sensitivity to $w_g$ depends on vegetation attenuation. In spring 2009, the Le Mona site was covered by a dense rapeseed crop, whereas in 2010 it was covered by wheat (relatively sparse at this period of the year). This explains that despite higher $w_g$ values in 2009, the observed $T_b$ are within the same range of the ones of 2010.

### 3.2. From CAROLS $T_b$ to $w_g$ using a dual configuration regression

Table 3 presents the results obtained for the 34H0H, 34V0V and 34VH configurations with $T_{eff}$ estimated using the first Eq. (2) formulation. Figure 7 illustrates the results of the 34VH configuration. This configuration presents the best scores, with only three sites (of 14) with non significant *p*-values (>0.05). These three sites correspond to forested areas, in the Les Landes forest (SBR site) and in a hilly area of Corbières (MTM). Regarding stations with significant statistical scores, the correlations and RMSE scores range from 0.50 to 0.93 and from 0.015 to 0.044 $m^3m^{-3}$, respectively. For 34H0H, the correlations tend to be lower than for 34VH, for several stations. Moreover, the use of the biangular configuration is limited for two stations close to strong RFI zones, PRG and CDM, which are affected by residual interferences, as shown by the high fraction of missing data for these two stations (Table 2): 84% and 77%, respectively, against an average value of 49% for all the stations. Indeed, the nadir $T_b$ at these stations are often higher than $T_{eff,}$ and this can be explained by residual RFI levels. Only 4 flights for CRD site and 6 flights for CDM site are found to be suitable to produce the score. This is not enough to obtain significant regressions. The 34V0V configuration is the less efficient, with six sites presenting non-significant correlations.

Table 4 presents the $A_{wg}$, $B_{wg}$ and $C_{wg}$ regression coefficient values of the dual-configuration regression method used in this study. They vary from a configuration to another and seem to be site specific. They may depend on the soil and vegetation properties acting on the microwave emission, like soil roughness, surface infiltration and thermal properties, vegetation phenology and canopy structure. Observed soil characteristics such as organic matter, clay and sand fractions, bulk density, are available for SMOSMANIA (Albergel et al., 2008). The link between the $A_{wg}$, $B_{wg}$ and $C_{wg}$ regression coefficients and the above mentioned characteristics was investigated (not shown). However no significant link between regressions coefficient and soil characteristics could be established.

### 3.3. Application to SMOS brightness temperatures

The $A_{wg}$, $B_{wg}$ and $C_{wg}$ regression coefficients determined for CAROLS's measurements were applied to these SMOS $T_b$ data previously filtered for RFI. The scores between the retrieved $w_g$ from SMOS and observed soil moisture are presented in Table 5. For eight stations of the SMOSMANIA network the correlations are significant ($p$-value <0.05) with $r$ and RMSE ranging from 0.25 to 0.60 and from 0.03 to 0.09 $m^{-3}m^{-3}$, respectively. The best scores ($p$-value <0.001) are obtained for SBR, MNT, and SFL (Fig. 8). Correlations are significant for the Le Mona, Lahage and Berat sites, also. The average RMSE value for all the significant correlations is 0.06$m^{-3}m^{-3}$ which is similar to the RMSE obtained with the ASCAT surface soil moisture products over the same sites (Albergel et al. 2009).

## 4. Discussion

This study investigated the sensitivity of CAROLS's L-band $T_b$ to soil moisture, over various landscape types. The dual configuration regression method used by Calvet et al. (2011) to assess the sensitivity to soil moisture was applied to the CAROLS biangular and bipolarized observations. The regression coefficients obtained for the 34VH configuration were applied to the SMOS $T_b$, also. The results obtained over three sites URG, LHS and SVN (Table 5) show no sensitivity to soil moisture (non-significant correlations). However, Albergel et al. (2009) and Albergel et al. (2010), found good correlations between in situ surface soil moisture observations at these sites and the ASCAT product. The lack of consistency between the

SMOS and the ASCAT or CAROLS results over some SMOSMANIA sites may be explained by:

- scale issues inducing discrepancies between the environment of the local in situ observations and the area of the size of a SMOS footprint around them,
- the presence of residual RFI in the SMOS $T_b$ dataset,
- the fact that the SMOS data are not reprocessed,
- the need to include more information into the regression equation (e.g. besides two polarizations, several contrasting incidence angles ; ancillary information about the vegetation opacity).

Whereas Saleh et al. (2010) suggested that the $A_{wg}$, $B_{wg}$ and $C_{wg}$ regression coefficients may depend on soil and vegetation characteristics, no significant link between regression coefficients and measured soil characteristics (such as soil texture, organic matter content, or dry density) could be established using the SMOSMANIA network. It must be noted that soil roughness (not measured) impacts $T_b$, also. The purpose of the manual measurements performed at Le Mona, Lahage, and Berat sites (close to the LHS SMOSMANIA station), was to test the representativeness of local observations. While the results presented in Fig. 7 show that soil moisture observations at these four sites are in the same range, the coefficients of the regressions Eq. (1b) markedly differ from one site to another (Table 3), in relation to contrasting vegetation, soil and relief characteristics. In particular, the Berat agricultural site presents a lower correlation than the other sites. Indeed, it is less representative of the area where distributed in situ measurements were taken, as it consisted of large flat maize fields with mainly bare soil in April and May, and rapidly growing maize in June.

Finally, as the coefficients of Eq. (1b) are derived from $T_b$ observations obtained at various dates, they implicitly represent the average vegetation impact on $T_b$ and the seasonal variation of vegetation properties, e.g. the vegetation water content (not measured). A consequence of the latter effect is that the values for the regression coefficients should not only be site specific but also show seasonal variation if computed separately for the main seasons. It is likely that the limited number of sites does not allow a robust analysis of the regression coefficients, and a modeling study with the version of the ISBA model able to simulate vegetation growth (Calvet et al. 1998) could help investigating this issue.

Correlations between CAROLS $T_b$ and in situ soil moisture are generally higher at nadir than at slant. A number of factors may explain this result. In particular, the area spotted by CAROLS at nadir is smaller than the one spotted at slant, and more representative of the in situ observations. Also, nadir observations are less affected by the vegetation opacity. Except for the PRG and CDM stations, presenting nadir observations affected by RFI, the Eq. (1b) regression using data at 34° at both polarizations yields results similar to the regressions using two angles at only one polarization. This is consistent with the results of Calvet et al. (2011), showing similar L-band soil moisture retrieval scores with one angle and two polarizations (30VH or 40VH), and two angles and one polarization (50V20V, 40V20V, 50H20H, 40H20H).

In addition to the RFI issue, the signal is influenced by the vegetation. A reduced sensitivity to soil moisture is to be expected over dense vegetation canopies. However, some stations, characteristic of highly vegetated agricultural areas (e.g. MNT) present very good scores. A possible explanation could be the presence of a significant fraction of bare soil and/or dry vegetation, caused by the crop rotation practices. This factor may explain the significant response of $T_b$ to soil moisture observed over agricultural areas, at L-band and, also, at higher frequencies (Calvet et al., 2011).

Regarding the SMOS data, two levels of products are distributed, brightness temperatures and soil moisture derived from the brightness temperatures. The soil moisture retrieval method is based on the $\tau$-$\omega$ model associated to a soil emission model, inverted through optimization methods (Pellarin et al. 2003a). This study confirms that simple regression methods (Pellarin et al. 2003b) are able to produce satisfactory results over a given set of sites. Even if $A_{wg}$, $B_{wg}$ and $C_{wg}$ regression coefficients seem to be site specific, the triplets of coefficients derived from the CAROLS data were successfully applied to the SMOS brightness temperatures.

# 5. Conclusions

This study provides several insights into the sensitivity to soil moisture of passive microwave observations at L-band. The performance of simple logarithmic statistical regression equations relating $w_g$ to the microwave emissivity was used as an indicator of this sensitivity. The CAROLS L-band observations were found to be very sensitive to soil moisture in the different configurations tested. Once converted to $w_g$ using simple logarithmic statistical regression equations, the retrieved $w_g$ present good correlations with observations. The application of the regression coefficients determined from the CAROLS emissivities to the SMOS emissivities showed promising results and a more in-depth analysis of this method is needed. The use of CAROLS L-band measurements and their confrontation to observed soil moisture is a first step before the evaluation of the SMOS products, to be reiterated when future reprocessed data become available.

## Acknowledgements

The work of C. Albergel was supported by Centre National d'Etudes Spatiales (CNES) and Météo-France. The work of E. Zakharova was supported by the STAE (Sciences et Technologies pour l'Aéronautique et l'Espace) foundation, in the framework of the CYMENT project. The CAROLS project was funded by the "Programme Terre Océan Surface

Continentales et Atmosphère” (TOSCA, CNES). The ATR-42 aircraft was operated by the SAFIRE UMS 2859.

# References

Albergel, C., Rüdiger, C., Pellarin, T., Calvet, J.-C., Fritz, N., Froissard, F., Suquia, D., Petitpa, A., Piguet, B., & Martin, E. (2008). From near-surface to root-zone soil moisture using an exponential filter: an assessment of the method based on in-situ observations and model simulations. *Hydrol. Earth Syst. Sci.*, *12*, 1323–1337. doi:10.5194/hess-12-1323-2008.

Albergel, C., Calvet, J.-C., de Rosnay, P., Balsamo, G., Wagner, W., Hasenauer, S., Naemi, V., Martin, E., Bazile, E., Bouyssel, F., & Mahfouf, J.-F. (2010). Cross-evaluation of modelled and remotely sensed surface soil moisture with in situ data in southwestern France, *Hydrol. Earth Syst. Sci.*, *14*, 2177-2191. doi:10.5194/hess-14-2177-2010.

Albergel, C., Rüdiger, C., Carrer, D., Calvet, J.-C., Fritz, N., Naeimi, V., Bartalis, Z., & Hasenauer, S. (2009). An evaluation of ASCAT surface soil moisture products with in-situ observations in southwestern France. *Hydrol. Earth Syst. Sci.*, *13*, 115-124. doi:10.5194/hess-13-115-2009.

Calvet, J.-C., Noilhan, J., Roujean, J.-L., Bessemoulin, P., Cabelguenne, M., Olioso, A., & Wigneron, J.-P. (1998). An interactive vegetation SVAT model tested against data from six contrasting sites. *Agric. For. Meteorol.*, *92*, 73–95, 1998.

Calvet, J.-C., Fritz, N., Froissard, F., Suquia, D., Petitpa, A., & Piguet, B. (2007). In situ soil moisture observations for the CAL/VAL of SMOS: the SMOSMANIA network. *Proceedings of the International Geoscience and Remote Sensing Symposium, IGARSS*, Barcelona. doi: 10.1109/IGARSS.2007.4423019.

Calvet, J.-C., Wigneron, J.-P., Walker, J., Karbou, F., Chanzy, A., & Albergel, C. (2011). Sensitivity of passive microwave observations to soil moisture and vegetation water content: L-band to W band. *IEEE Trans. Geosci. Remote. Sens.*, 49(4), 1190 – 1199, doi :10.1109/TGRS.2010.2050.488.

Chanzy, A., Schmugge, T. J., Calvet, J.-C., Kerr., Y, van Oevelen, P., Grosjean, O., & Wang, J.R. (1997). Airborne microwave radiometry on a semi arid area during Hapex-sahel. *J. Hydrol., 188-189*, 285-309.

Choudhury, B. J., Schmugge, T. J., & Mo, T. (1982). A parameterization of effective soil temperature for microwave emission. *J. Geophys. Res., 87, C2*, 1301–1304.

Dirmeyer, P.A., Dolman, A.J., & Sato, N. (1999). The pilot phase of the global soil wetness project. *Bull. Amer. Meteorol. Soc., 80*, 851-878.

Georgakakos, K.P., & Carpenter, M. (2006). Potential value of operationally available and spatially distributed ensemble soil water estimates for agriculture. *J. Hydrol., 328*, 177-191.

Habets, F., Ducrocq, V., & Noilhan, J. (2005). Prévisions hydrologiques et échelles spatiales: l'exemple des modèles opérationnelles de Météo-France, *C. R. Geoscience, 337*, 181–192.

Habets F., Boone, A., Champeaux, J.-L., Etchevers, P., Franchisteguy, L., et al. (2008). The SAFRAN-ISBA-MODCOU hydrometeorological model applied over France, *J. Geophys. Res., 113*, D06113, doi:10.1029/2007JD008548.

Jackson, T.J., Hsu, A.Y., van de Griend, A., & Eagleman, J.R. (2004). Skylab L band microwave radiometer observations of soil moisture revisited, *Int. J. Remote Sens., 25*, 2585-2606.

Kerr, Y., Waldteufel, P., Wigneron, J.-P., Martinuzzi, J.-M., Font, J., & Berger, M. (2001). Soil moisture retrieval from space: the soil moisture and ocean salinity (SMOS) mission, *IEEE Trans. Geosci. Remote. Sens., 39*, 1729–1736.

Kerr Y., Waldteufel, P., Richaume, P., Davenport, I., Ferrazzoli, P., & Wigneron, J.-P. (2007). SMOS level 2 processor soil moisture algorithm theoretical basis document

(ATBD), CESBIO, Toulouse, France. SM-ESL (CBSA), SO-TN-ESL-SM-GS-0001, ESA Internal report, V2.a., http://www.cesbio.ups-tlse.fr/us/indexsmos.html

Kerr, Y. (2007). Soil moisture from space: where are we? *Hydrogeol. J., 15(1),* 117–120.

Lemaître, F., Poussière, J. K., Kerr, Y. H., Déjus, M., Durbe, R., De Rosnay, P., & Calvet, J.-C. (2004). Design and test of the ground based L-band radiometer for estimating water in soils (LEWIS). *IEEE Trans. Geosci. Remote. Sens., 42*, 8, 1666-1676.

Njoku, E. G., Jackson, T. J., Lakshmi, V., Chan, T. K., & Nghiem, S. V. (2003). Soil moisture retrieval from AMSR-E, *IEEE Trans. Geosci. Remote. Sens., 41(2),* 215–123.

Njoku, E. G., Ashcroft, P., Chan, T. K., & Li, L. (2005). Global survey and statistics of radio-frequency interference in AMSR-E land observations, *IEEE Trans. Geosci. Remote. Sens.*, 43, 938-947.

Pardé, M., Zribi, M., Fanise, P., & Dechambre, M. (2011). Analysis of RFI issue using the CAROLS L-band experiment, *IEEE Trans. Geosc. Remote Sens., 49 (3),* 1063-1070.

Pellarin, T., Wigneron, J.-P., Calvet, J.-C., & Waldteufel, P. (2003a). Global soil moisture retrieval from a synthetic L-band brightness temperature data set. *J. Geophys. Res*., *108, D12*, 4364. doi : 10.1029/2002JD003086.

Pellarin, T., Calvet, J.-C., & Wigneron, J.-P. (2003b). Surface Soil Moisture Retrieval from L-band radiometry: a Global Regression Study. *IEEE Trans. Geosc. Remote Sens., 41*, 9, 2037-2051.

Rüdiger, C., Calvet, J.-C., Gruhier, C., Holmes, T., De Jeu, R., & Wagner, W. (2009). An intercomparison of ERS-Scat and AMSR-E soil moisture observations with model simulations over France. *J. Hydrometeorol., 10(2),* 431–447. doi:10.1175/2008JHM997.1

Saleh, K., Wigneron, J.-P., de Rosnay, P., Calvet, J.-C., & Kerr, Y. (2006). Semi empirical regression s at L-Band applied to surface soil moisture retrieval over grass. *Remote Sens. Environ., 101 (3)*, 415-426.

Schmugge, T. J. (1983). Remote sensing of soil moisture: recent advances, *IEEE Trans. Geosc. Remote Sens., GE21*, 145–146.

Schmugge, T. J., & Jackson, T.J. (1994). Mapping soil moisture with microwave radiometers, *Meteorol. Atmos. Phys., 54*, 213-223.

Skou, N. (1989). Microwave radiometer systems: design and analysis. MA, Norwood, USA: Artech House.

Wagner, W., Lemoine, G., & Rott, H. (1999). A method for estimating soil moisture from ERS scatterometer and soil data. *Remote Sens. Environ., 70*, 191-207.

Wagner, W., Naeimi, V., Scipal, K., de Jeu, R., & Martinez-Fernandez, J. (2007). Soil moisture from operational meteorological satellites, *Hydrogeol. J., 15*, 121–131.

Wagner, W., Blöschl, G., Pampaloni, P., Calvet, J.-C., Bizzarri, B., Wigneron, J.-P., & Kerr, Y. (2007). Operational readiness of microwave remote sensing of soil moisture for hydrologic applications. *Nord. Hydrol., 38(1)*, 1–20. doi:10.2166/nh2007.029.

White, I., Knight, J. H., Zegelin, S. J., & Topp, G. C. (1994). Comments on “Considerations on the use of time-domain reflectometry (TDR) for measuring soil water content”, by Whalley, W. R., Response, *Eur. J. Soil Sci., 45(4)*, 503–510.

Wigneron, J.-P., Chanzy, A., Calvet, J.-C., & Bruguier, N. (1995). A simple algorithm to retrieve soil moisture and vegetation biomass using passive microwave measurements over crop fields. *Remote Sens. Environ.,51 (3)*, 331-341.

Wigneron, J.-P., Calvet, J.-C., Pellarin, T., Van de Griend, A., Berger, M., & Ferrazzoli, P. (2003). Retrieving near surface soil moisture from microwave observations: Current status and future plan. *Remote Sens. Environ., 85, (4)*, 489-506.

Wigneron, J.-P., Calvet, J.-C., de Rosnay, P., Kerr, Y., Waldteufel, P., Saleh, K., Escorihuela, M.J., & Kruszewski, A. (2004). Soil moisture retrievals from biangular L-Band passive microwave observations, *IEEE Geosci. Remote Sens. Lett., 1 (4)*, 277-281.

Wigneron, J.-P., Chanzy, A., de Rosnay, P., Rüdiger, C., &Calvet, J.-C. (2008). Estimating the effective soil temperature at L-band as a function of soil properties, *IEEE Trans. Geosc. Remote Sens., 46 (3)*, 797-801.

Wilson, W. J., Yueh, S. H., Dinardo, S. J., Chazanoff, S. L., Kitiyakara, A., Li, F. K., & Rahmat-Samii, Y. (2001). Passive active L- and S-Band (PALS) microwave sensor for ocean salinity and soil moisture measurements, *IEEE Trans. Geosc. Remote Sens.*, 39, 5, 1039-1048.

Zribi, M., Pardé, M., Boutin, J., Fanise, P., Hauser, D., Dechambre, M., Kerr, Y., Leduc-Leballeur, M., Skou, M., Søbjærg, S.S., Albergel, C., Calvet, J.-C., Wigneron, J.-P., Lopez-Baeza, E., Ruis, A., & Tenerelli, J. (2011). CAROLS: a new airborne L-band radiometer for ocean surface and land observations. *Sensors, 11*, 719-742. doi:10.3390/s110100719.

# Tables

Table 1: Description of the 24 flights (6 in 2009 and 18 in 2010) performed during the CAROLS campaigns and taken in consideration in this study. Other flights performed over Spain are not used here.

| Date | Flight plan | Additional in situ measurements |
|---|---|---|
| 2009 April 28 | SMOSMANIA transect | YES |
| 2009 May 15 | SMOSMANIA transect | YES |
| 2009 May 18 | Gulf of Biscay | NO |
| 2009 May 20 | Gulf of Biscay | NO |
| 2009 May 26 | Gulf of Biscay | NO |
| 2009 May 27 | SMOSMANIA transect | YES |
| 2010 April 15 | SMOSMANIA transect | YES |
| 2010 April 28 | SMOSMANIA transect | YES |
| 2010 May 03 | SMOSMANIA transect | NO |
| 2010 May 06 | Gulf of Biscay | NO |
| 2010 May 08 | Gulf of Biscay | NO |
| 2010 May 09 | SMOSMANIA transect | NO |
| 2010 May 11 | Gulf of Biscay | NO |
| 2010 May 19 | Gulf of Biscay | NO |
| 2010 May 21 | SMOSMANIA transect | NO |
| 2010 May 26 | SMOSMANIA transect | YES |
| 2010 May 31 | SMOSMANIA transect | NO |
| 2010 June 04 | SMOSMANIA transect | NO |
| 2010 June 08 | SMOSMANIA transect | YES |
| 2010 June 13 | SMOSMANIA transect | NO |
| 2010 June 18 | SMOSMANIA transect | YES |
| 2010 June 22 | SMOSMANIA transect | NO |
| 2010 June 26 | SMOSMANIA transect | NO |
| 2010 July 01 | SMOSMANIA transect | YES |

Table 2: Correlations between CAROLS $T_b$ (in four configurations, nadir and slant antennas, at both H and V polarization) and $w_g$ using the pooled 2009-2010 data set. The fraction of data removed from the analysis (of the 2010 flights), as suspected to be contaminated by radio-frequency interferences, is indicated (right column).

| Station | CAROLS $T_b$ at nadir (0°) | | | CAROLS $T_b$ at 34° | | | Fraction of missing data (%) |
|---|---|---|---|---|---|---|---|
| | V pol. | H pol. | N | V pol. | H pol. | N | |
| SBR | -0,526 | -0,529 | 24 | -0,338 | -0,241 | 24 | 69 |
| URG | -0,754 | -0,738 | 24 | -0,269 | -0,660 | 24 | 34 |
| CRD | -0,810 | -0,760 | 24 | -0,198 | -0,495 | 24 | 31 |
| PRG | -0,867 | -0,865 | 24 | -0,240 | -0,737 | 24 | 84 |
| CDM | -0,780 | -0,878 | 24 | -0,299 | -0,610 | 24 | 77 |
| LHS | -0,728 | -0,724 | 24 | -0,233 | -0,545 | 24 | 34 |
| SVN | -0,805 | -0,814 | 24 | -0,169 | -0,523 | 24 | 36 |
| MNT | -0,870 | -0,862 | 22 | -0,410 | -0,655 | 22 | 36 |
| SFL | -0,730 | -0,728 | 17 | -0,361 | -0,701 | 18 | 39 |
| MTM | -0,691 | -0,667 | 17 | -0,494 | -0,606 | 18 | 48 |
| LZC | / | / | / | / | / | / | 52 |
| NBN | -0,815 | -0,795 | 17 | -0,251 | -0,578 | 18 | 35 |
| **AVERAGE** | **-0,761** | **-0,760** | / | **-0,297** | **-0,577** | / | **49** |
| | | | | | | | |
| Le Mona | -0,811 | -0,801 | 9 | -0,161 | -0,986 | 9 | 36 |
| Lahage | -0,882 | -0,886 | 9 | -0,361 | -0,882 | 9 | 39 |
| Berat | -0,819 | -0,794 | 9 | -0,101 | -0,752 | 9 | 45 |
| **AVERAGE** | **-0,837** | **-0,827** | / | **-0,208** | **-0,873** | / | **40** |

Table 3: Comparison between observed and retrieved $w_g$, from biangular and bipolarization CAROLS configurations (34H0H, 34V0V, 34VH), for the 14 soil moisture observation sites used in this study, using the 17 SMOSMANIA transect flights (Table 1). Correlation coefficients, root mean square error (RMSE, in units of $m^3m^{-3}$) and *F*-Test *p*-values are presented. In the right column, two observation numbers are indicated for PRG and CDM stations: the number of valid observations for (left) 34H0H and 34V0V configurations and (right) 34VH. NS (non significant), *, **, ***, **** stand for *p*-values greater than 0.05, between 0.05 and 0.01, between 0.01 and 0.001, between 0.001 and 0.0001 and below 0.0001, respectively.

| | 34H0H | | | 34V0V | | | 34VH | | | *n* |
|---|---|---|---|---|---|---|---|---|---|---|
| | *r* | RMSE | *p*-value | *r* | RMSE | *p*-value | *r* | RMSE | *p*-value | |
| SBR | 0.50 | 0.015 | NS | 0.49 | 0.014 | NS | 0.50 | 0.015 | NS | 17 |
| URG | 0.81 | 0.048 | *** | 0.69 | 0.051 | ** | 0.86 | 0.044 | *** | 17 |
| CRD | 0.74 | 0.017 | ** | 0.72 | 0.018 | ** | 0.73 | 0.018 | ** | 17 |
| PRG | 0.60 | / | NS | 0.59 | 0.025 | NS | 0.84 | 0.021 | ** | 4/13 |
| CDM | 0.49 | 0.021 | NS | 0.42 | 0.019 | NS | 0.77 | 0.022 | ** | 6/15 |
| LHS | 0.63 | 0.033 | * | 0.57 | 0.032 | NS | 0.67 | 0.034 | * | 17 |
| SVN | 0.68 | 0.034 | * | 0.62 | 0.033 | * | 0.68 | 0.034 | * | 17 |
| MNT | 0.93 | 0.015 | **** | 0.87 | 0.019 | **** | 0.93 | 0.015 | **** | 17 |
| SFL | 0.75 | 0.027 | ** | 0.72 | 0.027 | ** | 0.71 | 0.027 | * | 17 |
| MTM | 0.58 | 0.014 | NS | 0.57 | 0.014 | NS | 0.53 | 0.013 | NS | 17 |
| LZC | / | / | / | / | / | / | / | / | / | / |
| NBN | 0.77 | 0.021 | ** | 0.70 | 0.021 | ** | 0.85 | 0.019 | *** | 17 |
| Le Mona | 0.92 | 0.029 | ** | 0.83 | 0.038 | * | 0.88 | 0.034 | * | 9 |
| Lahage | 0.92 | 0.022 | ** | 0.91 | 0.023 | ** | 0.90 | 0.024 | ** | 9 |
| Berat | 0.77 | 0.025 | NS | 0.71 | 0.025 | NS | 0.70 | 0.025 | NS | 9 |

Table 4: $A_{wg}$, $B_{wg}$ and $C_{wg}$ regression coefficients from the multiple configuration regression method applied to CAROLS data.

| | $A_{wg}$ | | | $B_{wg}$ | | | $C_{wg}$ | | |
|---|---|---|---|---|---|---|---|---|---|
| | 34H0H | 34V0V | 34VH | 34H0H | 34V0V | 34VH | 34H0H | 34V0V | 34VH |
| SBR | 0.135 | 0.142 | 0.107 | -0.001 | -0.011 | 0.029 | 0.414 | 0.442 | 0.425 |
| URG | 0.743 | 0.603 | 1.703 | -0.134 | -0.134 | -1.000 | 1.720 | 1.567 | 1.663 |
| CRD | 0.127 | 0.110 | 0.155 | 0.024 | 0.020 | -0.010 | 0.447 | 0.446 | 0.425 |
| PRG | 0.109 | 0.044 | 0.715 | 0.006 | 0.008 | -0.272 | 0.533 | 0.433 | 1.019 |
| CDM | 0.089 | 0.034 | 0.636 | 0.015 | 0.018 | -0.257 | 0.595 | 0.512 | 0.957 |
| LHS | 0.181 | 0.109 | 0.563 | 0.010 | 0.031 | -0.300 | 0.658 | 0.620 | 0.648 |
| SVN | 0.338 | 0.265 | 0.640 | -0.085 | -0.083 | -0.332 | 0.674 | 0.660 | 0.637 |
| MNT | 0.218 | 0.206 | 0.315 | 0.009 | 0.011 | -0.095 | 0.832 | 0.901 | 0.779 |
| SFL | 0.150 | 0.141 | 0.161 | 0.033 | 0.032 | 0.018 | 0.620 | 0.660 | 0.617 |
| MTM | 0.034 | 0.036 | 0.040 | 0.014 | 0.015 | 0.002 | 0.333 | 0.355 | 0.318 |
| LZC | / | / | / | / | / | / | / | / | / |
| NBN | 0.123 | 0.091 | 0.468 | -0.009 | -0.007 | -0.291 | 0.443 | 0.433 | 0.396 |
| Le Mona | 2.569 | -0.415 | 0.852 | -1.956 | 0.666 | -0.472 | 1.048 | 0.687 | 0.770 |
| Lahage | -1.085 | -0.078 | 0.270 | 1.255 | 0.354 | 0.025 | 0.801 | 0.806 | 0.824 |
| Berat | -1.726 | -0.025 | 0.087 | 1.719 | 0.199 | 0.086 | 0.460 | 0.530 | 0.542 |

Table 5 : Comparison between observed and retrieved $w_g$, from SMOS brightness temperatures, using the $A_{wg}$, $B_{wg}$ and $C_{wg}$ regression coefficients from the CAROLS 34VH configuration.

| | 34VH | | | |
|---|---|---|---|---|
| | *r* | RMSE ($m^3m^{-3}$) | *p*-value | *n* |
| SBR | 0.37 | 0.032 | *** | 96 |
| URG | 0.14 | 0.117 | NS | 44 |
| CRD | 0.25 | 0.043 | * | 90 |
| PRG | 0.4 | 0.059 | ** | 61 |
| CDM | 0.32 | 0.057 | ** | 75 |
| LHS | 0.14 | 0.073 | NS | 63 |
| SVN | 0.25 | 0.091 | NS | 57 |
| MNT | 0.43 | 0.089 | **** | 107 |
| SFL | 0.60 | 0.061 | **** | 97 |
| MTM | 0.30 | 0.037 | * | 68 |
| NBN | 0.29 | 0.044 | * | 55 |

## Figures

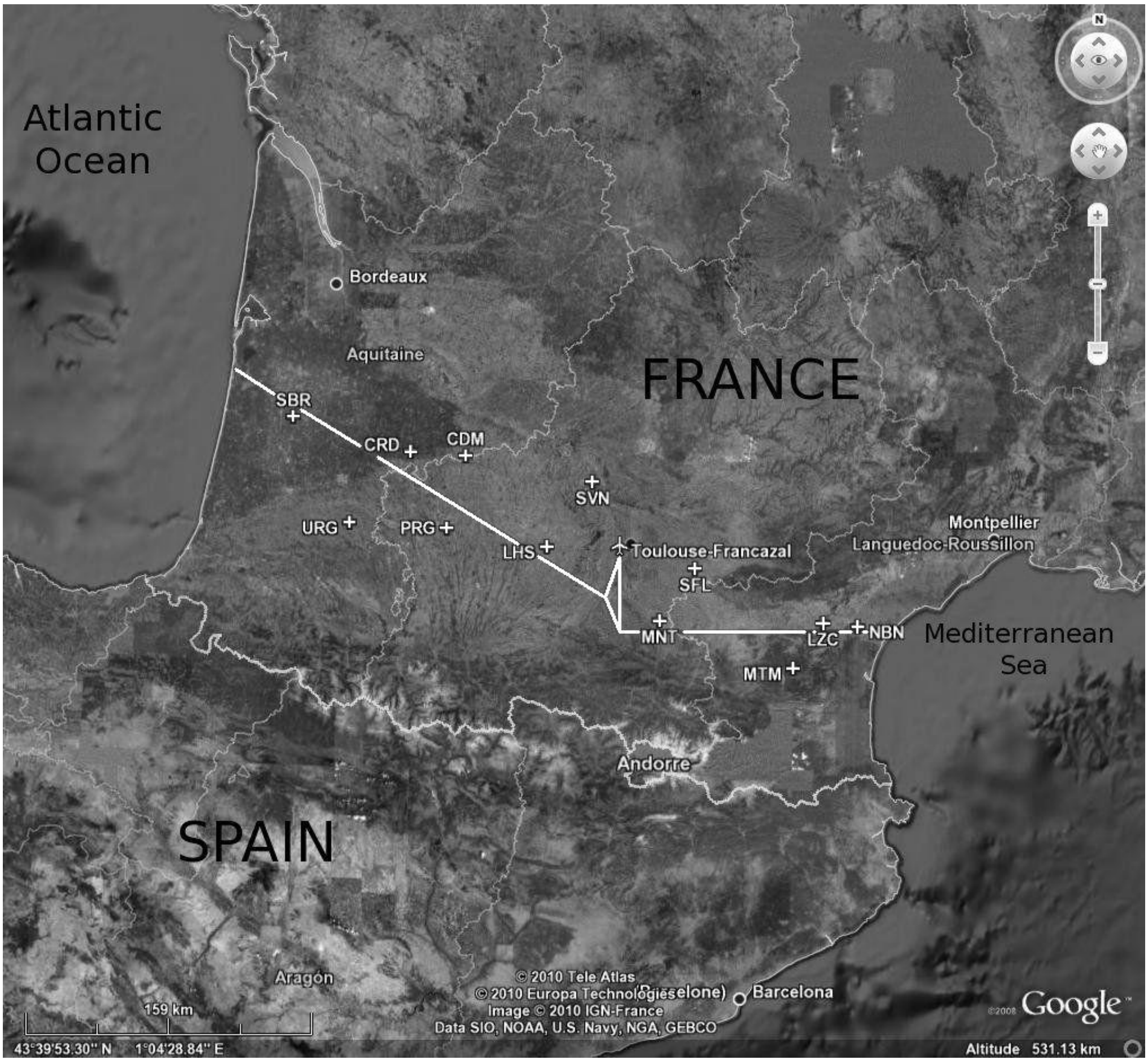


Figure 1: Map illustrating the SMOSMANIA network located in southwestern France (white crosses) forming a 400 km transect between the Atlantic ocean and the Mediterranean Sea. The stations are equipped with sensors measuring volumetric soil moisture content at various depth. The white line is for the CAROLS flights.

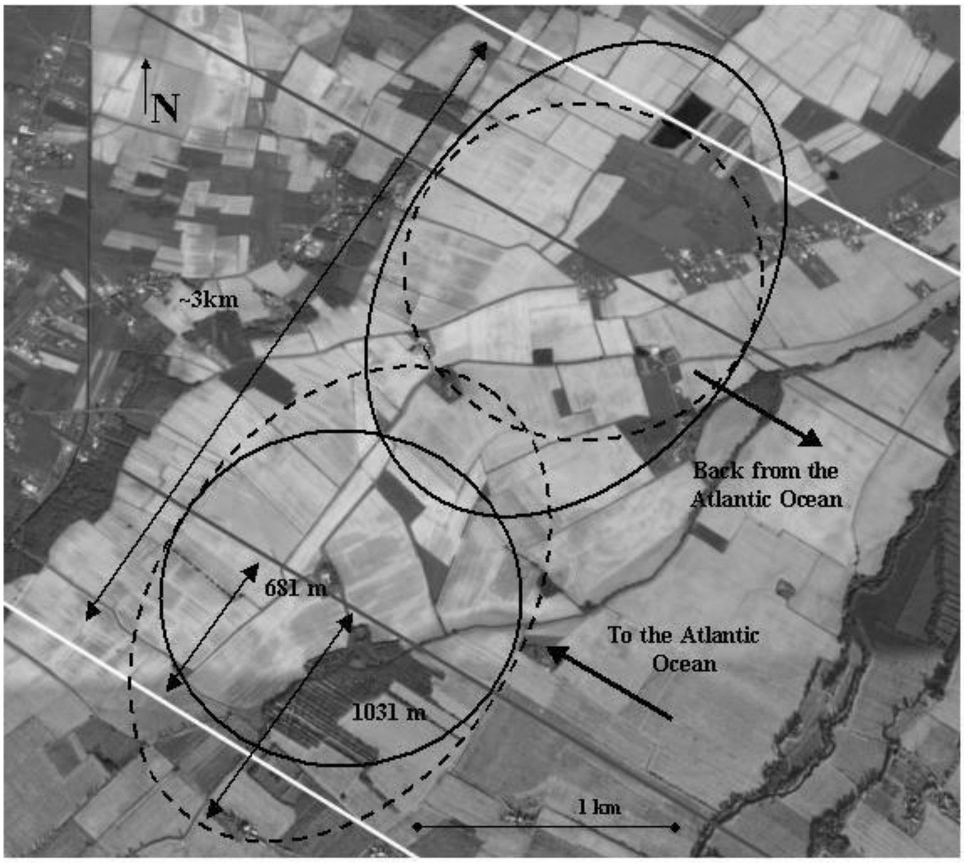


Figure 2: Schematic view of the surface at the Berat site, observed by the CAROLS instrument during a flight, at 2000m asl.

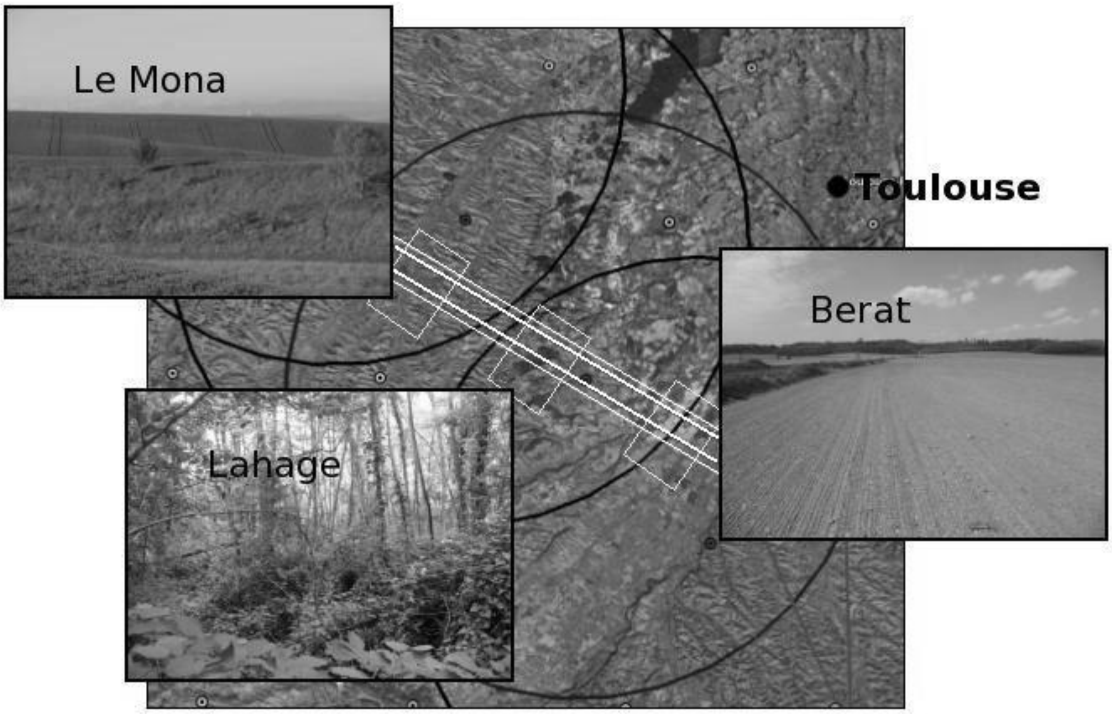


Figure 3: Three additional sites (white boxes) within a SMOS pixel (circles), at the southwest of Toulouse (black dot), investigated together with the twelve stations of the SMOSMANIA network. In situ soil moisture measurements at these three sites are performed with manual ThetaProbes. White lines are for the CAROLS flights.


Figure 4 : Illustration of soil moisture acquisition on the Le Mona site for 2010 April 28. Soil moisture is measured with ThetaProbes by two teams (yellow and red line).

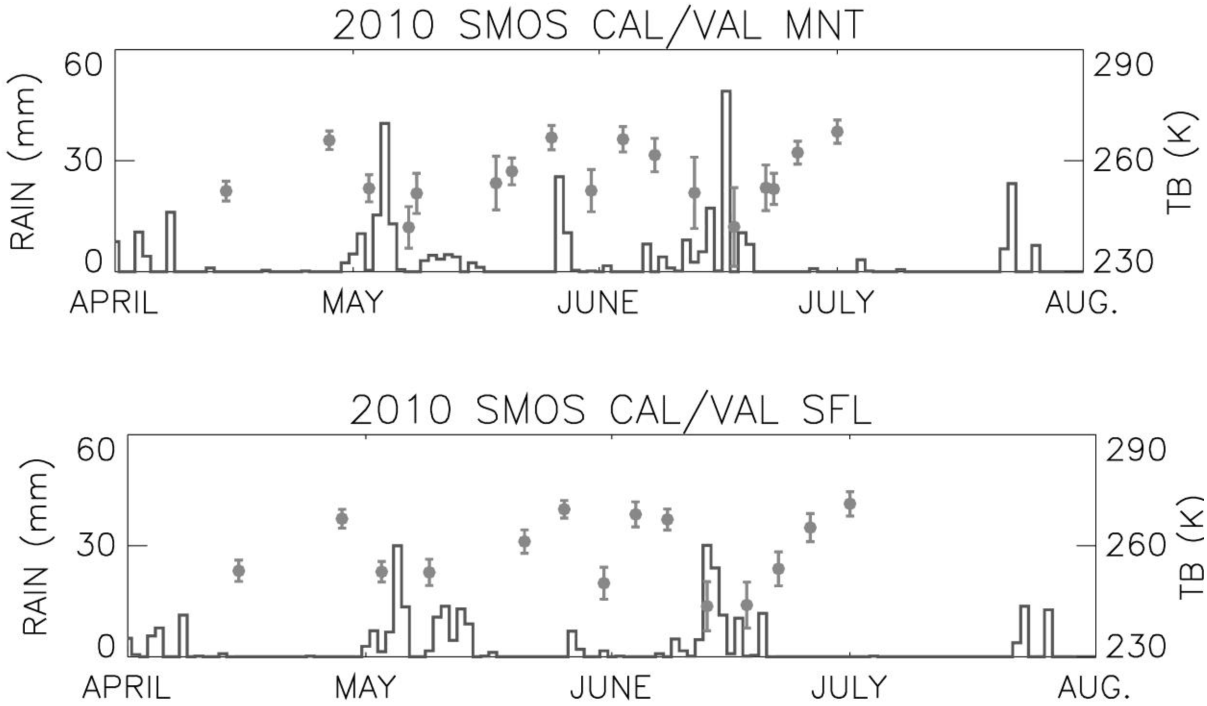


Figure 5: CAROLS's microwave $T_b$ observations (dots) at nadir (0°) in vertical polarization (V) with errors bars (standard deviation) for two stations of the SMOSMANIA network: Montaut (MNT) and Saint-Felix de Lauragais (SFL). The observed rain is also presented (line).

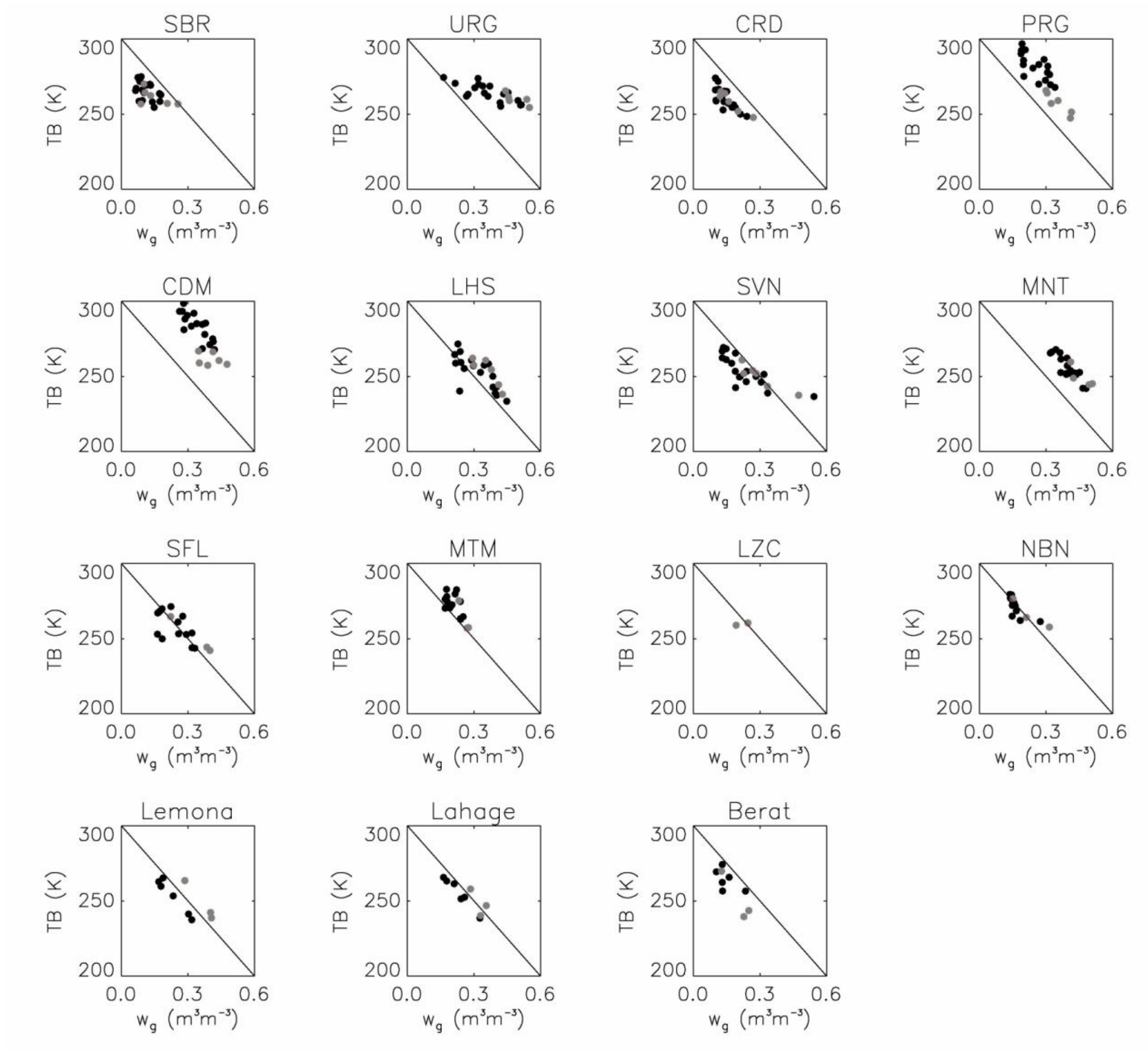


Figure 6 : CAROLS's microwave observations (nadir 0°, vertical V polarization) as a function of the in situ soil moisture at 5cm, for 2009 (grey dots) and 2010 (black dots).

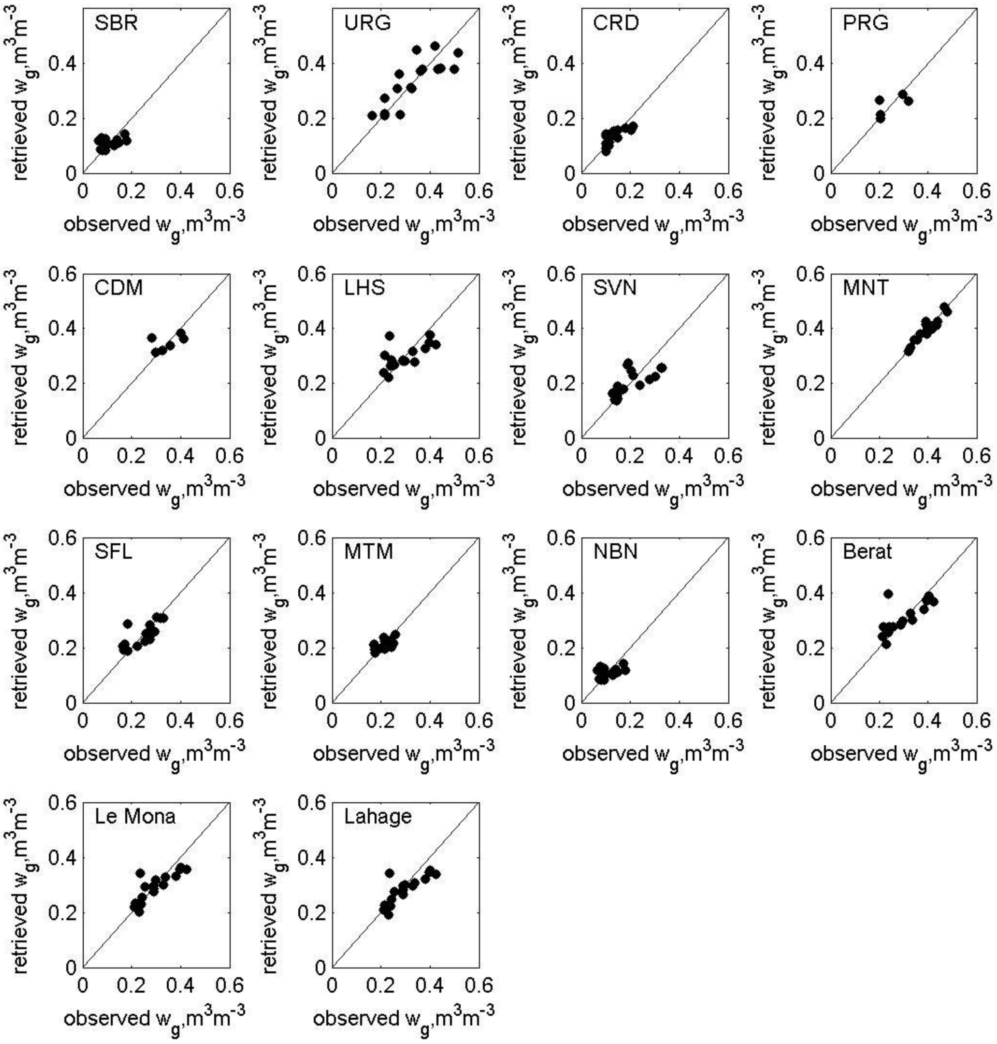


Figure 7: Retrieved versus observed $w_g$ using the CAROLS brightness temperatures in the 34VH bipolarized regression, for the 14 soil moisture observations sites. There are no in situ observations at the LZC station for the considered period.

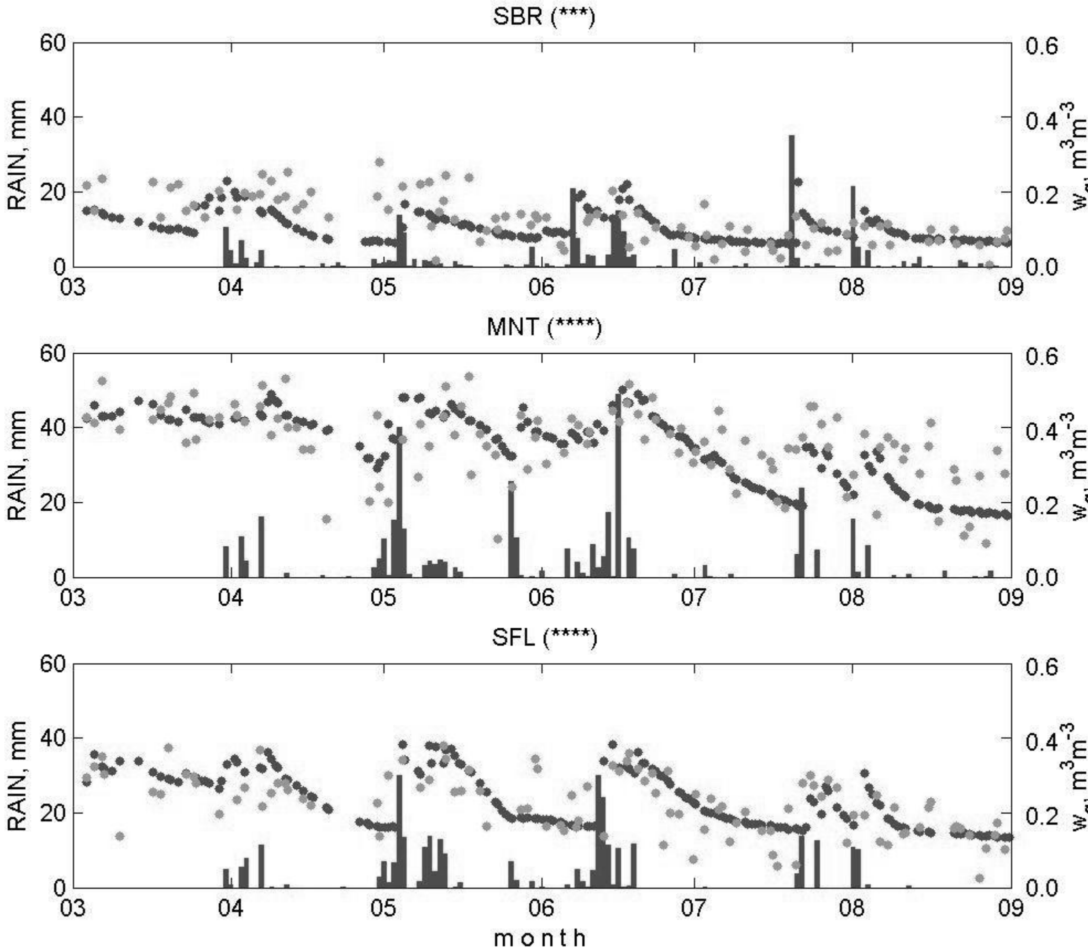


Figure 8: Time series of surface soil moisture ($w_g$) retrieved from SMOS $T_b$ using CAROLS empirical coefficients with the bipolarized approach (34HV), and observed in situ at three SMOSMANIA stations, from March to September 2010. From top to bottom: Sabres (SBR), Montaut (MNT), and Saint-Felix de Lauragais (SFL). Daily precipitation is represented by vertical bars. Black dots are for the in situ $w_g$, and grey dots for SMOS-derived $w_g$. The level of correlation significance between observed and retrieved $w_g$ is given in brackets

**Figure 1**
Click here to download high resolution image

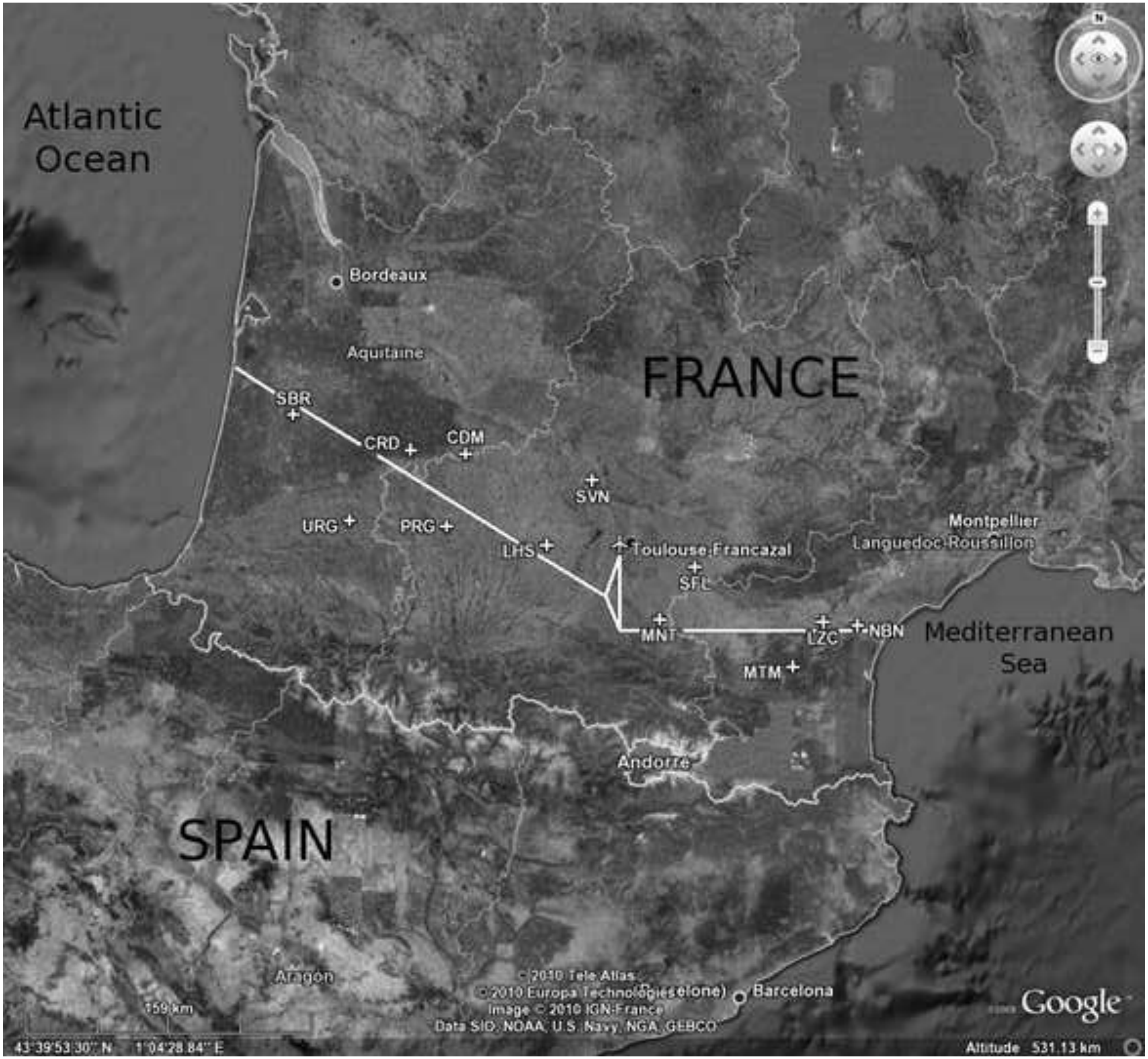

Figure 2
Click here to download high resolution image

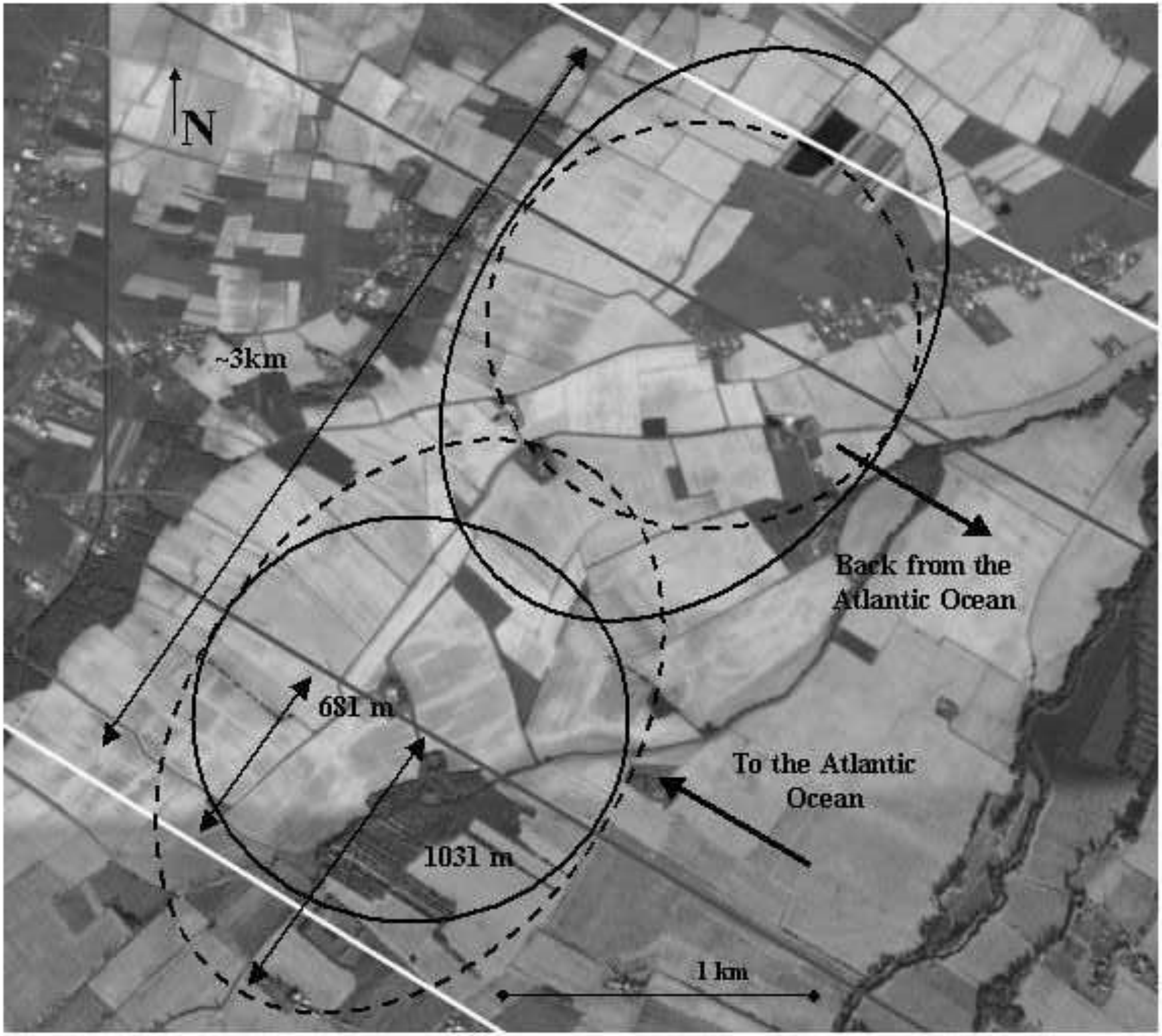

Figure 3
Click here to download high resolution image

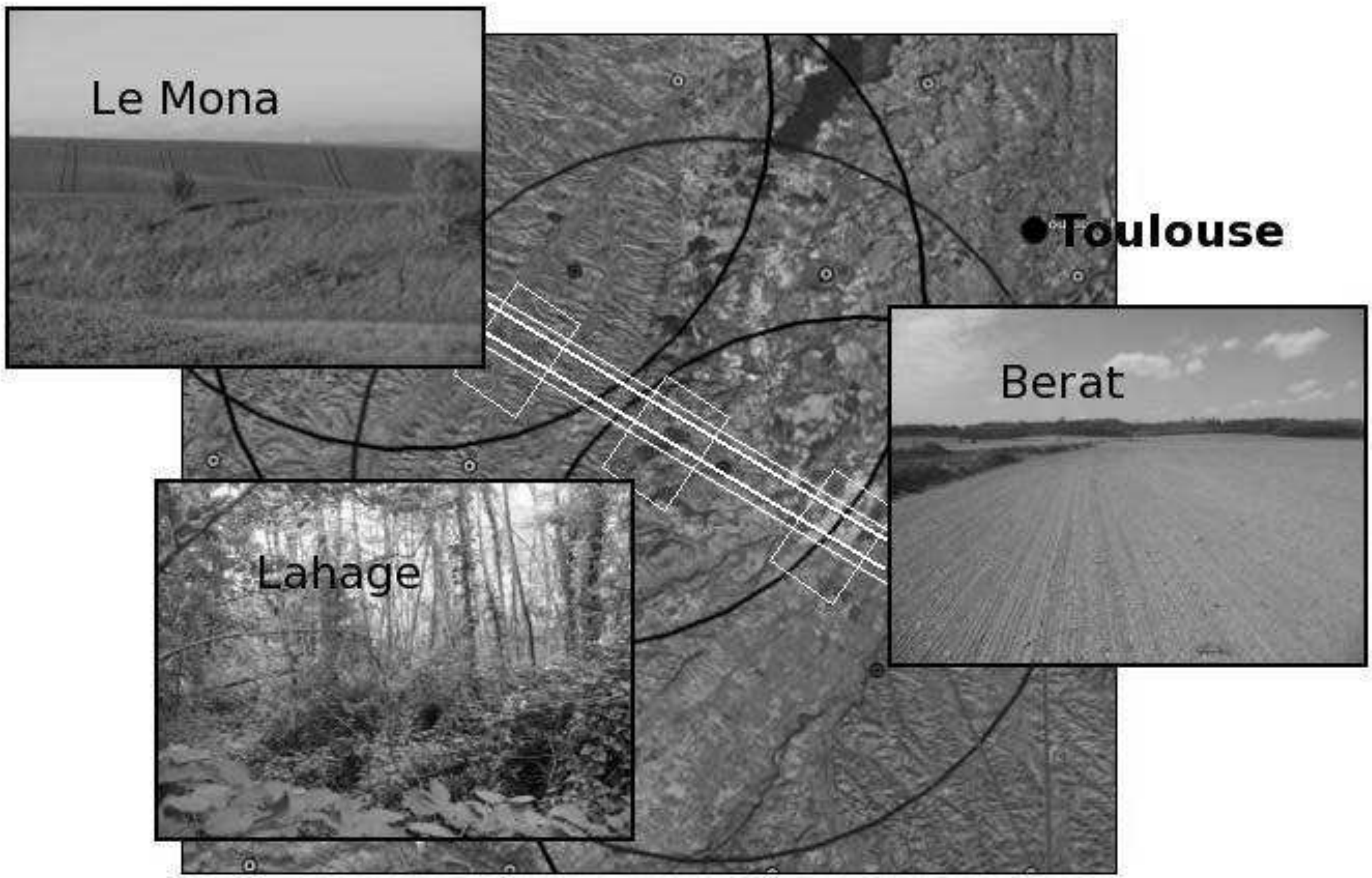

Figure 4
Click here to download high resolution image

Figure 5

Click here to download high resolution image

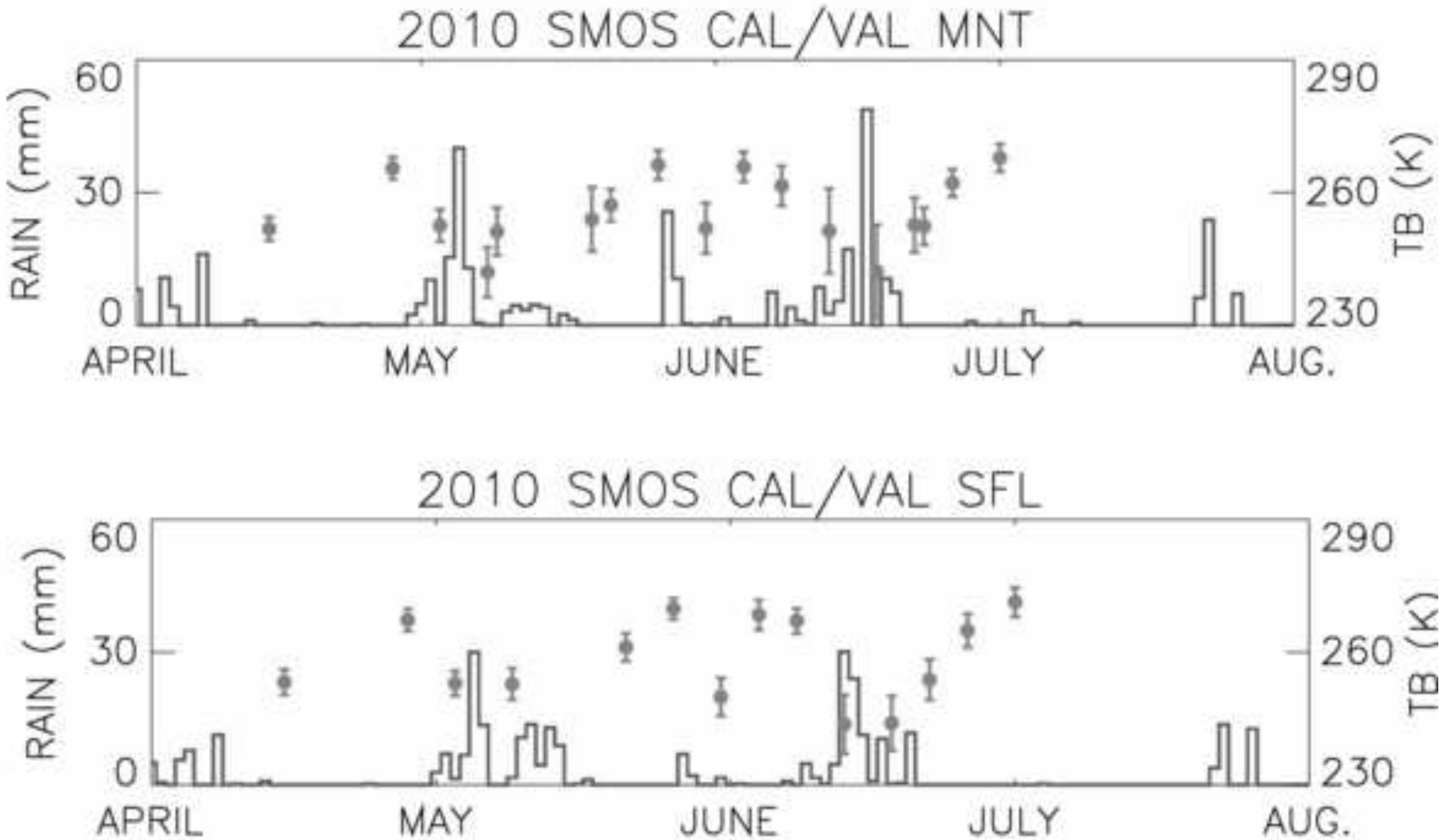

Figure 6

Click here to download high resolution image

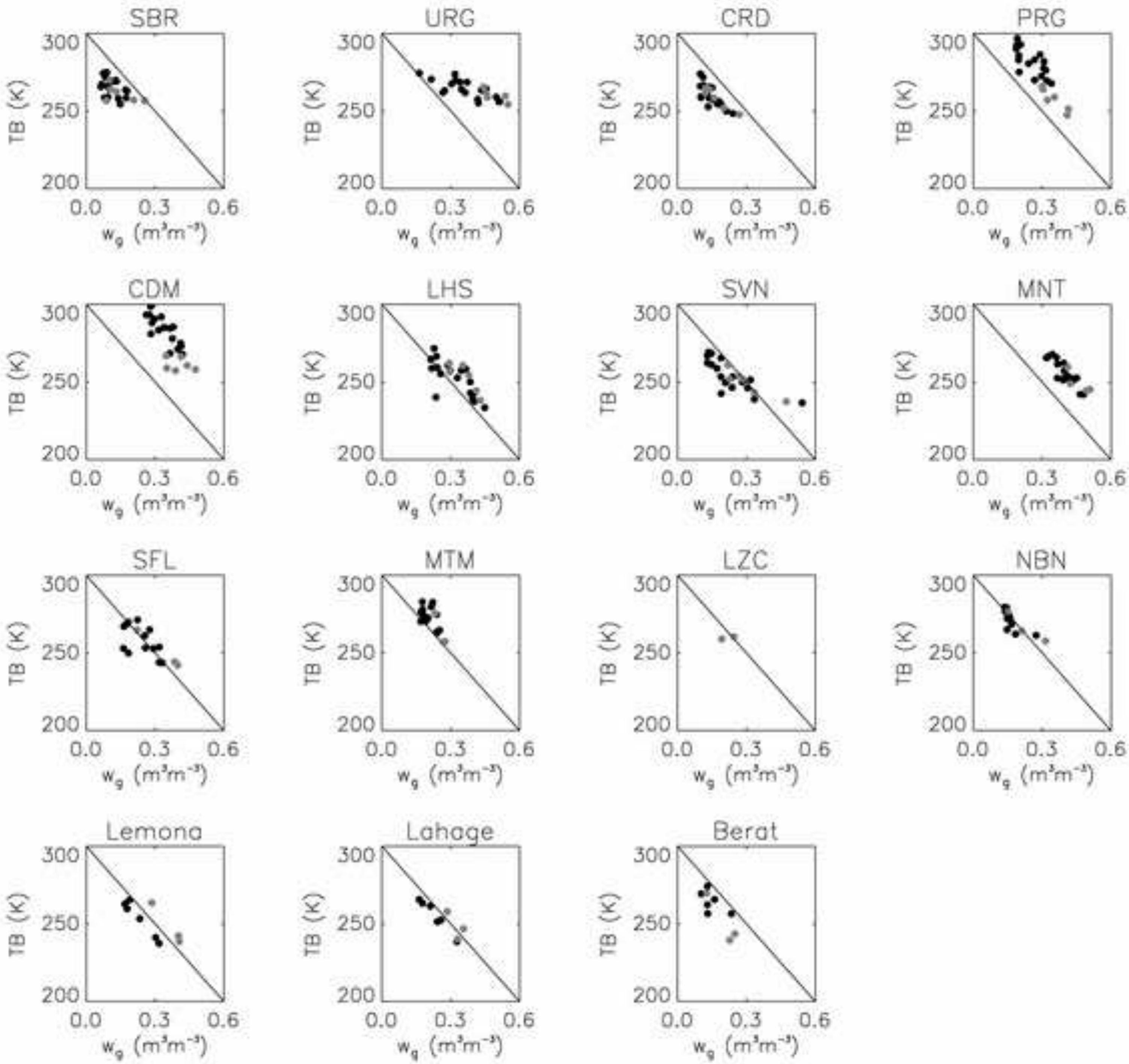

Figure 7

Click here to download high resolution image

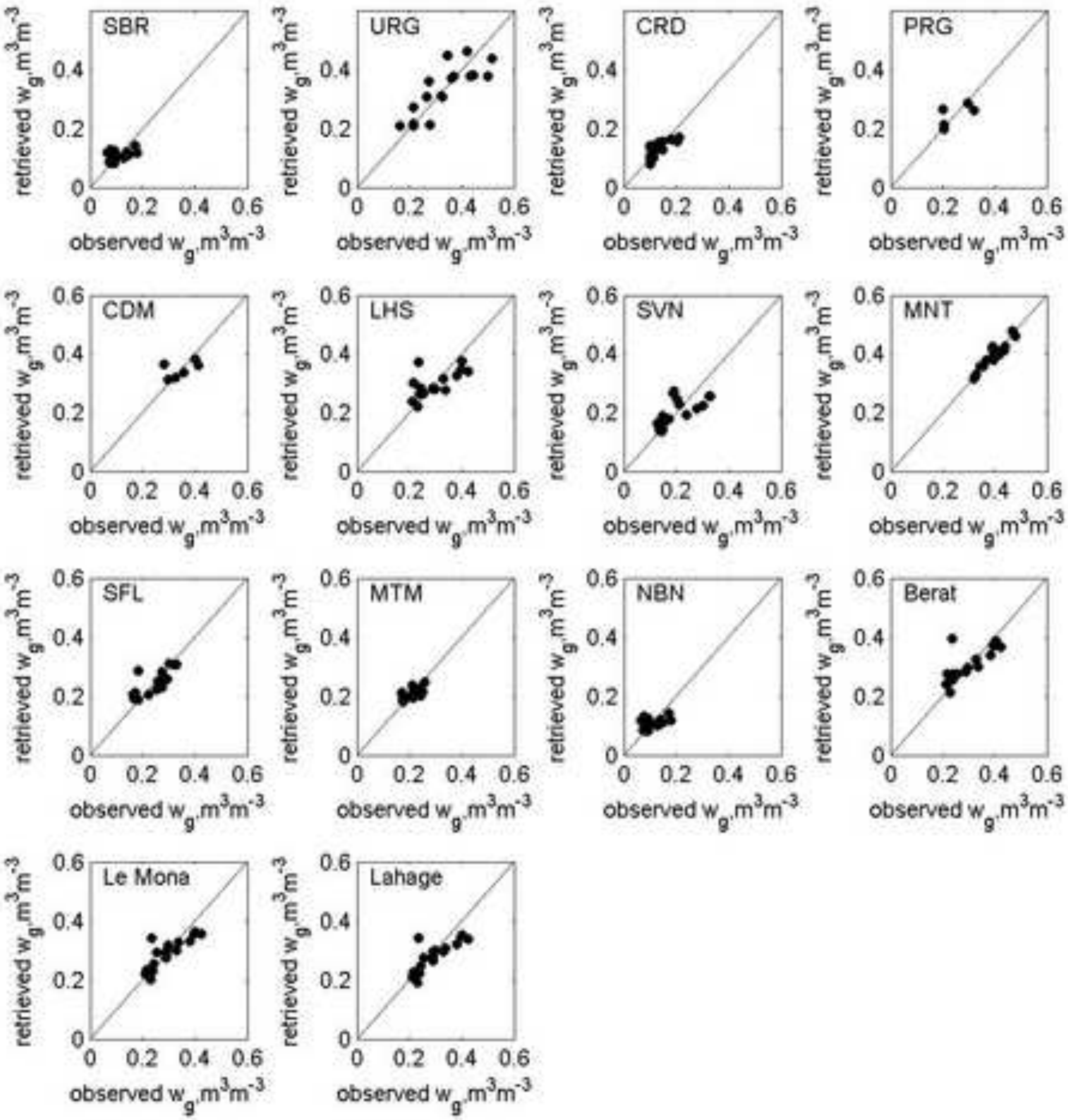

Figure 8

Click here to download high resolution image